Received: 15 May 2024 | Revised: 8 August 2024 | Accepted: 8 August 2024

DOI: 10.1002/pamm.202400079

PAMM Proceedings in Applied Mathematics and Mechanics

RESEARCH ARTICLE

Data-driven simulation of functional fatigue in shape memory alloy wires

Marius Harnisch[1] | **Thorsten Bartel**[1] | **Lukas Weyergraf**[1] | **Andreas Menzel**[1,2] | **Ben Schweizer**[3]

[1]Institute of Mechanics, Department of Mechanical Engineering, TU Dortmund, Dortmund, Germany

[2]Division of Solid Mechanics, Department of Construction Sciences, Lund University, Lund, Sweden

[3]Department of Mathematics, TU Dortmund, Dortmund, Germany

Correspondence
Marius Harnisch, Institute of Mechanics, Department of Mechanical Engineering, TU Dortmund, Germany.
Email: marius.harnisch@udo.edu

Funding information
German Research Foundation, Grant/Award Number: 440942664; Vetenskapsradet, Grant/Award Number: 2022-03460

Abstract
Data-driven mechanics offers great potential in engineering applications, where the efficient simulation of complex and, in particular, path-dependent material behavior is often challenging. Within this approach, conventional material models are replaced by data sets containing snapshots of stress, strain and the history of both assumed to be sufficiently accurate representations of the underlying material behavior. Based on these snapshots and on physical admissibility, a distance function is built which is minimized to yield the boundary value problems' solution. The aim of this paper is to apply this framework to accurately simulate the complex behavior of shape memory alloy wires under cyclic loading, under which these materials exhibit a degradation of their features, denoted functional fatigue. The constructed synthetic data sets are enriched by real experimental data, showcasing that the data-driven method is capable of combining both approaches of classic material modeling and modern methods which directly incorporate experimental data.

1 | INTRODUCTION

Scientific research in recent years has increasingly prioritized methods which directly incorporate the information governed in data. In solid mechanics and particularly in material modeling, their ongoing deployment is driven by the challenge to efficiently integrate complex modeling concepts into global computational schemes such as the finite element method (FEM) – even for purely elastic behavior. Within data-based methods, a new scheme is established in ref. [1] in which discrete data is incorporated directly into computational mechanics. Denoted data-driven mechanics, the method replaces material models by a data set containing snapshots of stress and strain assumed to be sufficiently accurate representations of the underlying material behavior. Within the data-driven scheme a distance is constructed based on these snapshots, referred to as material states, and on states fulfilling equilibrium of forces and kinematic compatibility, denoted mechanical states. The aim is to minimize this distance with respect to both states yielding the boundary value problems' solution.

The concept has since undergone significant development: In ref. [2], an approach to construct a constitutive manifold based on material states is presented. Additionally, in ref. [3] a maximum-entropy formulation of the data-driven approach is developed, enhancing its robustness against outliers and noisy data. A comprehensive discussion of the entire framework required for data-driven methods, covering aspects from experimental design to computational analyses, is provided in ref. [4]. Taking a different perspective on the concept, the Data-Driven Identification Method is proposed in ref. [5], which addresses the inverse problem by identifying a dataset of stress and strain based on known mechanical strains and boundary conditions.

To facilitate broader applications of data-driven mechanics, extending it to encompass inelastic material behavior is a crucial step. A first approach is presented in ref. [6] featuring a hybrid approach establishing local histories of the material states fixed to the material points. The approach presented in ref. [7] pursues a different direction, using structured data sets enriched by local tangents in phase space. The transition between multiple of these structured sets is decided by transition rules based on yield functions. In refs. [8] and [9], an extension to path-dependent material behavior is presented, in which the spirit of the original approach is preserved by enhancing the local distance function such that the results are still obtained via global minimization. Thereby, no real-time adjustments of the data set are necessary.

In the contribution at hand, we aim to utilize this scheme and to deploy it to simulate the complex material behavior of shape memory alloy (SMA) wires under cyclic loading, demonstrating a specific application of this approach. To be specific, these materials exhibit a degradation of their features under cyclic loading, including a change of the hysteresis' shape resulting in a decrease of the recoverable strains and transformation stresses. This degradation is denoted functional fatigue and is mainly credited to an interaction between plasticity occurring at the phase front and phase transformations, compare ref. [10]. Furthermore, experimental stress-strain data for SMA wires is available in literature and we directly incorporate the experimental results reported in ref. [11] into our data set, which otherwise contains synthetic data generated via the model provided in ref. [10].

The paper is structured as follows: In Section 2, we briefly revisit our extension of the data-driven approach to path-dependent material behavior. In Section 3, we discuss the data set creation incorporating the functional fatigue behavior of SMA wires. We present data-driven results in Section 4 and compare them to both the experimental data and the material model. We summarize our work in Section 5 and provide a conclusion.

2 | DATA-DRIVEN INELASTICITY

Our extension, compare ref. [12], of the data-driven algorithm will be presented for spatially two-dimensional truss structures where the local states in each truss are one-dimensional, resulting in scalar-valued stresses and strains. A quantity denoted history surrogate $\underline{\mathcal{H}}$ is introduced, in which the essential information of the history path of the material is stored. Indicated by the notation used (underlining), this quantity is vector-valued in the discretized setting. The extension is based on the double minimization problem

$$\min_{\left(\underline{B}^e\underline{u}_k,\sigma_k^e\right)\in\mathcal{E}_{\mathrm{enh},k}} \ \min_{(\tilde{\varepsilon},\tilde{\sigma},\underline{\tilde{\mathcal{H}}})\in\mathcal{D}_{\mathrm{enh}}} \ d^2_{\mathrm{enh}}(\mathcal{E}_{\mathrm{enh},k},\mathcal{D}_{\mathrm{enh}}) \tag{1}$$

subject to the constraints

$$\underline{f}_{\mathrm{ext},k} - \sum_{e=1}^{n_{\mathrm{el}}} A^e\, l^e \sigma_k^e\, [\underline{B}^e]^{\mathrm{t}} = \underline{0} \tag{2}$$

$$\underline{u}_k = \underline{\bar{u}}_k \tag{3}$$

where d_{enh} is an enhanced version of the distance function introduced in ref. [1]. The vector $\underline{f}_{\mathrm{ext},k}$ contains prescribed forces at the trusses' nodes, $\underline{B}^e$ is an operator which encodes the geometry of the underlying truss system and reflects the discrete gradient of the displacement field $\underline{u}_k$, A^e is the cross-section of element e, l^e its length, and $\underline{\bar{u}}_k$ contains prescribed displacements at the nodes of the trusses. The total number of truss elements is given by n_{el}. The mechanical states at time $t = t_k$ are given in discrete form

$$\mathcal{E}_{\mathrm{enh},k} := \left\{ \left(\underline{B}^e\underline{u}_k, \sigma_k^e, \underline{\mathcal{H}}_{k-1}^e\right) \quad \text{subject to} \quad (2) \text{ and } (3) \right\} \tag{4}$$

and in addition $\mathcal{D}_{\mathrm{enh}} := \left\{(\tilde{\varepsilon},\tilde{\sigma},\underline{\tilde{\mathcal{H}}})_1,(\tilde{\varepsilon},\tilde{\sigma},\underline{\tilde{\mathcal{H}}})_2,\dots,(\tilde{\varepsilon},\tilde{\sigma},\underline{\tilde{\mathcal{H}}})_{n_D}\right\}$ is the discrete data set containing a total of n_D material states. Within each time instance $t_k \in \{0 = t_0 < t_1 < t_2 < \cdots < t_K = T\}$ with the total number of steps $K \in \mathbb{N}$ and total time $T \in \mathbb{R}$, the objective is to find those pairs of strain and stress $(\varepsilon_k^e = \underline{B}^e\, \underline{u}_k, \sigma_k) \in \mathcal{E}_{\text{enh},k}$, which are closest to the entries of the data set $\mathcal{D}_{\text{enh}}$ in the sense of strain ε_k^e, stress σ_k^e and current history $\underline{\mathcal{H}}_{k-1}^e$ by solving (1). The distance is defined on element level between the mechanical state $(\underline{B}^e\, \underline{u}_k, \sigma_k^e, \underline{\mathcal{H}}_{k-1}^e) \in \mathcal{E}_{\text{enh},k}$ of truss e and a specific material state $(\widetilde{\varepsilon}, \widetilde{\sigma}, \underline{\widetilde{\mathcal{H}}})_i \in \mathcal{D}_{\text{enh}}$ as

$$[d_{\text{enh}}^e]^2\Big((\underline{B}^e\, \underline{u}_k, \sigma_k^e, \underline{\mathcal{H}}_{k-1}^e), (\widetilde{\varepsilon}, \widetilde{\sigma}, \underline{\widetilde{\mathcal{H}}})_i\Big) := \frac{1}{2}\,\mathrm{E}\,(\underline{B}^e\, \underline{u}_k - \widetilde{\varepsilon}_i)^2 + \frac{1}{2}\,\mathrm{C}\,(\sigma_k^e - \widetilde{\sigma}_i)^2 + \frac{1}{2}\,\|\underline{\mathcal{H}}_{k-1}^e - \underline{\widetilde{\mathcal{H}}}_i\|_A \tag{5}$$

with $\|\underline{x}\|_A^2 := \underline{x}^{\mathrm{t}}\, \underline{A}\, \underline{x}$ and E and C being numerical parameters, whereas $\underline{A}$ is a diagonal matrix containing non-negative numerical parameters. Following the staggered solution approach proposed in ref. [1], first the closest material states $(\widetilde{\varepsilon}^{*e}, \widetilde{\sigma}^{*e}, \underline{\widetilde{\mathcal{H}}}^{*e})$ within each element $e = 1\, \ldots, n_{\text{el}}$ given fixed mechanical states, which are set to zero in the initial step, are found via

$$(\widetilde{\varepsilon}^{*e}, \widetilde{\sigma}^{*e}, \underline{\widetilde{\mathcal{H}}}^{*e}) = \arg \min_{(\widetilde{\varepsilon}, \widetilde{\sigma}, \underline{\widetilde{\mathcal{H}}})_i \in \mathcal{D}_{\text{enh}}} \Big\{ [d_{\text{enh}}^e]^2\Big((\underline{B}^e\, \underline{u}_k, \sigma_k^e, \underline{\mathcal{H}}_{k-1}^e), (\widetilde{\varepsilon}, \widetilde{\sigma}, \underline{\widetilde{\mathcal{H}}})_i\Big)\Big\}, \tag{6}$$

which define the current (fixed) material state of the truss structure $\mathcal{D}_{\text{enh}}^* := \Big\{ (\widetilde{\varepsilon}^{*e}, \widetilde{\sigma}^{*e}, \underline{\widetilde{\mathcal{H}}}^{*e}) \text{ with } e = 1, \ldots, n_{\text{el}} \Big\}$. Upon this solution a total distance is built, that is,

$$d_{\text{enh}}^2(\mathcal{E}_{\text{enh},k}, \mathcal{D}_{\text{enh}}^*) = \sum_{e=1}^{n_{\text{el}}} A^e\, l^e\, [d_{\text{enh}}^e]^2((\underline{B}^e\, \underline{u}_k, \sigma_k^e, \underline{\mathcal{H}}_{k-1}^e), (\widetilde{\varepsilon}^{*e}, \widetilde{\sigma}^{*e}, \underline{\widetilde{\mathcal{H}}}^{*e})), \tag{7}$$

which is minimized for a fixed material state, to be specific

$$(\underline{u}_k^*, \sigma_k^{*e}) = \arg\, \min\big\{ d_{\text{enh}}^2(\mathcal{E}_{\text{enh},k}, \mathcal{D}_{\text{enh}}^*)\big\} \quad \text{subject to} \quad (2) \text{ and } (3), \tag{8}$$

to obtain the updated strain $\varepsilon_k^{*e} = \underline{B}^e\, \underline{u}_k^*$ and stress σ_k^{*e} of the mechanical state, completing one iteration step of the staggered solution scheme. Finding the identical material state in two consecutive iterations terminates the algorithm. The iterated mechanical state solution is then utilized to find the history surrogate $\underline{\mathcal{H}}_k^e$ in each element via

$$\underline{\mathcal{H}}_k^e = \mathcal{P}(\varepsilon_k^{*e}, \sigma_k^{*e}, \underline{\mathcal{H}}_{k-1}^e), \tag{9}$$

where $\mathcal{P}$ is denoted as propagator. For the inelastic, one-dimensional case, the history surrogate can be specifically chosen according to ref. [12], that is,

$$\underline{\mathcal{H}}_{k-1}^e := \{\varphi_1, \tau_1, \rho_1, \ldots, \varphi_m, \tau_m, \rho_m, \ldots, \varphi_{n_{\text{lr}}}, \tau_{n_{\text{lr}}}, \rho_{n_{\text{lr}}}, \varepsilon, \sigma\}_{k-1}^e \tag{10}$$

where the triplet $(\varphi_m, \tau_m, \rho_m)^e$ reflects strain, stress, and an indicator value saved at load reversal no. m with $m = 1, \ldots, n_{\text{lr}}$, where $n_{\text{lr}} \in \mathbb{N}$ reflects a predetermined number of load reversals to be tracked. The two last values $(\varepsilon, \sigma)_{k-1}^e$ are the strain and stress of element e at time t_{k-1} and are used to detect a new load reversal. The history surrogate is initially set to zero $\underline{\mathcal{H}}_0^e \equiv \underline{0}$ in all elements and the triplet together with the two last entries of the history surrogate are updated via the propagator $\mathcal{P}$ according to the case distinction

$$\underline{\mathcal{H}}_k^e(\varphi_m, \tau_m, \rho_m, \varepsilon_{k-1}, \sigma_{k-1})^e = \begin{cases} (0, 0, \operatorname{sign}(\varepsilon_k^{*e}), 0, 0)\,,\ m = 1 & \text{for } \underline{\mathcal{H}}_{k-1}^e \equiv \underline{0} \wedge \varepsilon_k^{*e} \neq 0 \\ (\varphi_m^e, \tau_m^e, \rho_m^e, \varepsilon_k^{*e}, \sigma_k^{*e}) & \text{for } \rho_m^e \neq 0 \wedge \operatorname{sign}(\Delta\varepsilon) = \rho_m^e \wedge \Delta\varepsilon \neq 0 \\ (\varepsilon_{k-1}^e, \sigma_{k-1}^e, \operatorname{sign}(\Delta\varepsilon), \varepsilon_k^{*e}, \sigma_k^{*e})\,,\ m \leftarrow m+1 & \text{for } \rho_m^e \neq 0 \wedge \operatorname{sign}(\Delta\varepsilon) \neq \rho_m^e \wedge \Delta\varepsilon \neq 0 \\ \underline{\mathcal{H}}_{k-1}^e & \text{for } \Delta\varepsilon = 0 \end{cases} \tag{11}$$

with $\Delta\varepsilon := \varepsilon_k^{*e} - \varepsilon_{k-1}^e$. At the end of each time step it is checked for a new load reversal, and if none is detected, the history surrogate is updated with respect to the final two entries $(\varepsilon, \sigma)_{k-1}^e$. In case a load reversal is detected, the triplet

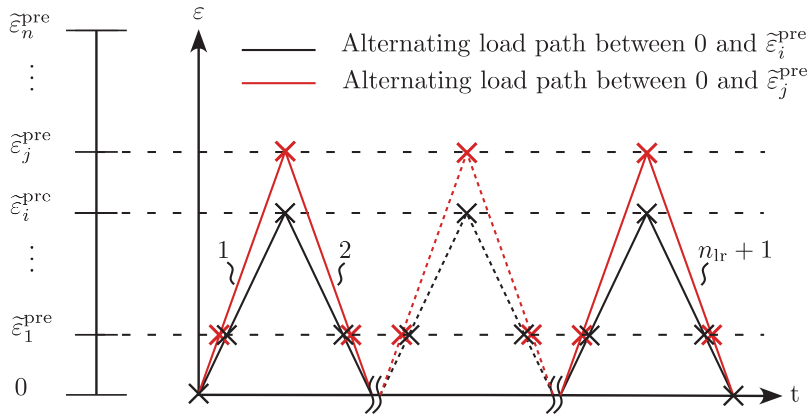

FIGURE 1 Schematic illustration of the data set generation. First (left) the strain space is sampled by prescribing a total of n strain values equidistantly in the regime $[0, \widetilde{\varepsilon}_1^{\text{pre}}, \widetilde{\varepsilon}_2^{\text{pre}}, \dots, \widetilde{\varepsilon}_n^{\text{pre}}]$. Then, a load path is generated for each of these values, where the load is alternated a total of $n_{\text{lr}}+1$ times between 0 and the prescribed strain value, in this example $\widetilde{\varepsilon}_i^{\text{pre}}$ (black) and $\widetilde{\varepsilon}_j^{\text{pre}}$ (red).

$(\varphi_m, \tau_m, \rho_m)^e$ is additionally updated at position m, whereas all previous triplets remain unchanged. This procedure is repeated until a total of n_{lr} load reversals have been detected and stored. The weight matrix $\underline{A}$ introduced in (5) is chosen as the diagonal matrix of size $(3\,n_{\text{lr}}+2)\times(3\,n_{\text{lr}}+2)$, where the first $3\,n_{\text{lr}}$ diagonal entries are given as the repeated arrangement of $(\mathrm{k}_\varphi, \mathrm{k}_\tau, \mathrm{k}_\rho)$ and the final two diagonal entries are given as $(\mathrm{k}_\varepsilon, \mathrm{k}_\sigma)$. All load reversals are therefore weighted equally.

3 | DATA GENERATION AND FUNCTIONAL FATIGUE IN SHAPE MEMORY ALLOY WIRES

This contribution aims to simulate the behavior of SMA wires at constant temperature as reported in ref. [11] via our data-driven extension. Therefore, load cycles are performed by exclusively alternating between 0 and some prescribed strain $\widetilde{\varepsilon}_i^{\text{pre}}$. We prescribe a total of $n \in \mathbb{N}^+$ of these strain values equidistantly in the regime $[0, \widetilde{\varepsilon}_1^{\text{pre}}, \widetilde{\varepsilon}_2^{\text{pre}}, \dots, \widetilde{\varepsilon}_n^{\text{pre}}]$, compare Figure 1, where we refer to n as the resolution of the strain sampling. In ref. [9], a data set construction for arbitrary load paths, including multiple load reversals, is presented. However, as stated above, it is sufficient to reduce the considered load paths to ones exclusively alternating between 0 and some prescribed strain $\widetilde{\varepsilon}_i^{\text{pre}}$, thereby reducing the amount of data tremendously. In order to do so, we modify the presented approach in ref. [9] to the extent that unloading is always performed to 0 and subsequent loading is always performed to the identical strain $\widetilde{\varepsilon}_i^{\text{pre}} \neq 0$ of previous load reversals of the same path, schematically visualized in Figure 1. The remaining techniques, which assure to also contain paths with less or no load reversals without saving redundant data, are utilized without modification. By doing so, simulations of truss structures, where individual truss elements have different strain paths, are still possible. The corresponding stress values are either taken from the experimental data in ref. [11] or otherwise are calculated based on the model in ref. [10]. Revisiting the fundamental equations of this model exceeds the scope of this contribution. A model itself is necessary to obtain synthetic data for load cycles that are not included in the experimental data. Ideally, the chosen model should be calibrated to the available experimental data. Table 1 provides the numerical and physical parameters chosen for the creation of this synthetic data. The resulting paths of stress and strain $(\widetilde{\varepsilon}_k, \widetilde{\sigma}_k)^{k=1,\dots,l_{\text{p}}}$ of length l_{p} are reduced to a single data set entry $(\widetilde{\varepsilon}, \widetilde{\sigma}, \underline{\mathcal{H}})_i$ utilizing the propagator $\mathcal{P}$ according to Section 2 and are saved in a global data set $\mathcal{D} := \left\{(\widetilde{\varepsilon}, \widetilde{\sigma}, \underline{\mathcal{H}})_1, (\widetilde{\varepsilon}, \widetilde{\sigma}, \underline{\mathcal{H}})_2, \dots, (\widetilde{\varepsilon}, \widetilde{\sigma}, \underline{\mathcal{H}})_{n_D}\right\}$ containing n_D entries.

4 | RESULTS

We perform single element simulations utilizing our data-driven approach for path-dependent material behavior based on the SMA data sets according to Section 3. We choose single element calculations as we focus on reproducing the material behavior and wish to exclude structural effects. Nevertheless, the data generation was designed such that it could also be

TABLE 1 Physical and numerical parameters used to create the synthetic data based on the model in ref. [10].

Parameter	Symbol	Value	Parameter	Symbol	Value
Wire diameter	A	$0.49\,\pi\,10^{-6}$ m^2	Viscosity-like parameter	γ	0.001 Ns/m^3
Wire length	L	0.1 m	Density	ρ	6.7×10^3 kg/m^3
Youngs modulus austenite	E_A	72×10^9 Pa	Specific heat capacity	c_M	453 J/kgK
Youngs modulus martensite	E_M	24×10^9 Pa	Damping coefficients	$\delta_{\mathrm{L}}, \delta_{\mathrm{Y}}, \delta_{X_\Gamma}$	0.15 [–]
Initial latent heat	$\mathrm{L}^{\mathrm{ini}}$	0.046×10^9 Pa	Reference temperature	θ_0	233.15 K
Saturated latent heat	$\mathrm{L}^{\mathrm{sat}}$	0.039×10^9 Pa	Transformation strain	$\varepsilon^{\mathrm{tr}}$	0.025 [–]
Initial dissipation coefficient	$\mathrm{Y}^{\mathrm{ini}}$	0.0375×10^9 Pa	Min. saturated phase front position	$X_{\Gamma_1}^{\mathrm{min,sat}}$	0.025 m
Saturated dissipation coefficient	$\mathrm{Y}^{\mathrm{sat}}$	0.0169×10^9 Pa			

TABLE 2 Data set numbering, used resolution n of the strain space and resulting total number of data set entries n_D.

No.	Resolution n	Data set entries n_D
1	5	974
2	10	1274
3	25	2174
4	50	73 549
5	100	297 099
6	150	670 649
7	200	1 194 199
8	250	1 882 440

used within the simulations of truss structures (as long as the maximum prescribed load is identical for each cycle and the prescribed load results in strains which are covered within the data). We create eight data sets including $n_{\mathrm{lr}} = 60$ load reversals (=30 load cycles) with increasing resolution of the strain sampling, compare Table 2. All data sets are created with a maximum strain of $\bar{\varepsilon}_n^{\mathrm{pre}} = 0.05$. For all simulations, the numerical weights in (5) are chosen to

$$\mathrm{E} = 72 \times 10^{10}, \quad \mathrm{C} = 1/\mathrm{E}, \quad \mathrm{k}_\varphi = 72 \times 10^{12}, \quad \mathrm{k}_\tau = 1/\mathrm{k}_\varphi, \quad \mathrm{k}_\rho = 1, \quad \mathrm{k}_\varepsilon = 0 \quad \text{and} \quad \mathrm{k}_\sigma = 0.$$

For both the data-driven calculations and the reference calculations via ref. [10], we use 12 000 time steps with a step size of $\Delta t = 0.005$ s.

We enriched our data sets via the data presented in ref. [11]. To verify that the data-driven solver is indeed capable of using the constructed data sets which merged this experimental data with synthetic data, we perform a first simulation, where the prescribed strain path matches the one utilized to obtain the experimental data. In this path, a total of 30 cycles are prescribed, where each cycle is loaded up to a maximum strain of $\varepsilon_{\mathrm{load}}^{\mathrm{max}} = 0.05$ and the time steps per cycle are distributed evenly. Figure 2 presents the obtained data-driven results for cycle no. 1, no. 5, and no. 30 utilizing data set no. 8. Within this plot, the experimental data itself is additionally visualized which acts as the reference to compare the stress-strain response against. It is remarked that only the experimental data for these cycles is available and the data set was filled with synthetic data elsewhere. As it can be observed in Figure 2, the data-driven solution accurately matches the experimental data. As the prescribed strain path is always unloaded to zero, the experimental data does not cover the complete unloading path. In this case, the data-driven solver resorts to the aforementioned synthetic data also included in the data set, providing an explanation for the observable kinks at the limit of the experimental data. Additionally, it is observable that the data-driven solution deviates from the experimental data for the first cycle. This is most likely due to the chosen number of time steps or numerical weights: The smaller the number of steps, the larger the prescribed strain increments. This may lead to the data-driven solver finding data set entries which better match these increments, even though their history surrogate might deviate slightly from the one of the mechanical state. In particular for the first cycle, where the history surrogate only contains a single reversal in load, the increased error in the history can be compensated by the reduced error of the current strain and stress. In consequence, this behavior is no longer observable for a rising number

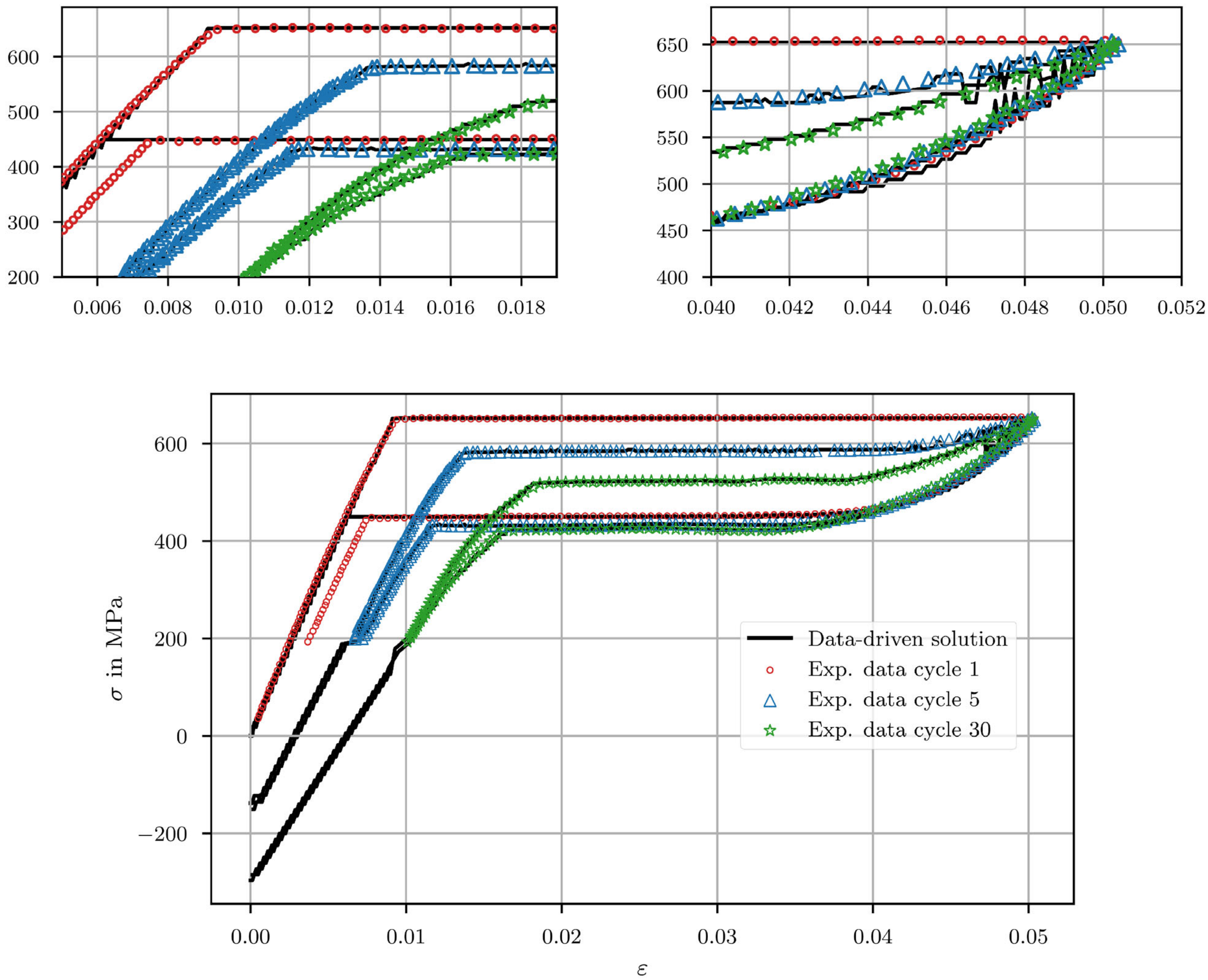

FIGURE 2 Qualitative comparison of data-driven solution obtained using data-set no. 8, compare Table 2, against the experimental data from ref. [11] for cycle no. 1, no. 5, and no. 30. Note, that only the experimental data for these cycles is available and elsewhere, the data set was filled with synthetic data.

of load cycles. Furthermore, increasing the number of time steps or adjusting the numerical weights should allow to fix this behavior even for the first cycle. These aspects should be considered and investigated in future work.

As mentioned before, the data generation presented in Section 3 may also be utilized for simulations of truss structures, where the maximum strain $\varepsilon_{\text{load}}^{\max}$ differs within each truss. Therefore, for the second example, we reuse the aforementioned numerical weights and parameters but prescribe a different maximum strain of $\varepsilon_{\text{load}}^{\max} = 0.035$. In Figure 3, the stress-strain response predicted by the data-driven algorithm (solid black line) is presented once again for cycle no. 1, no. 5, and no. 30 in conjunction with the material models response (colored lines), which acts as the reference solution for this case. The data-driven solution was calculated using data-set no. 8 and shows overall very good agreement with this reference solution, merely at the point of load reversal for cycle 30, a minor deviation is visible. Everywhere else, no deviation can be detected by naked eye. Supplementing this qualitative comparison, we conduct an additional quantitative comparison by utilizing a regularized mean squared error (RMSE) over all time steps, which is based on the error measure introduced in ref. [1]. We define this error to

$$\sigma^{\text{RMSE}} = \frac{1}{K}\sum_{k=1}^{K} \sigma_k^{\text{RMSE}} \quad \text{with} \quad \sigma_k^{\text{RMSE}} := \frac{1}{\sigma_{\text{ref}}^{\max}} \left[\left[\sigma_k^e - \sigma_{\text{ref}}^e \right]^2 \right]^{1/2}, \tag{12}$$

where $\sigma_{\text{ref}}^{\max}$ is the maximum absolute stress of the reference solution over all time steps k. Figure 4 shows the evolution of this error measure over the increasing density of the data sets used, compare Table 2. As expected, the error decreases

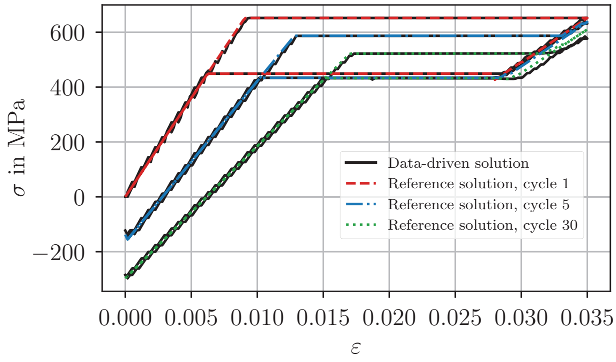

FIGURE 3 Qualitative comparison of the data-driven solution utilizing data set no. 8 and the response of the phenomenological model [10], acting as the reference solution, for cycle 1, 5, and 30.

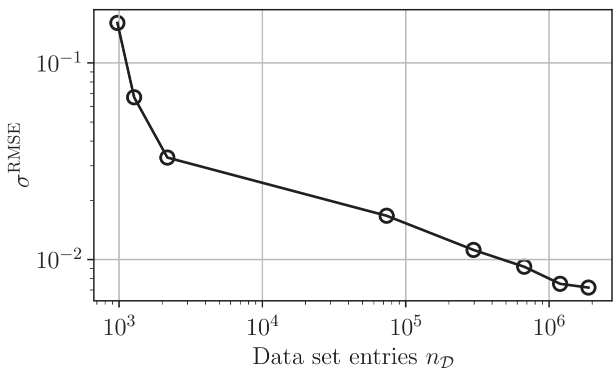

FIGURE 4 Quantitative comparison of the data-driven solution and the phenomenological model [10] acting as reference solution over all cycles according to (12) for the utilized data sets, compare Table 2.

with an increasing density. After an initially very steep decrease, a kink is noticeable at data set no. 3, after which the error continues to decrease steadily but not as steep as before. It is remarked that the error of data-set no. 3 of $\sigma^{\mathrm{RMSE}} \approx 0.033 = 3.3\%$ could already be considered sufficiently small for certain applications and scenarios. It is sufficient to only consider the error in the stress, because the error in the strain is (numerically) zero for a prescribed strain path.

5 | SUMMARY

With the extension of the data-driven method to path-dependent material behavior, compare [12], a broad range of applications becomes available. One of these being the simulation of functional fatigue behavior in SMA wires, where the data-driven method allows for a direct combination of data obtained by conventional material models and experimental data. While the synthetic data is generated based on the phenomenological model in ref. [10], the data set is additionally enriched by real experimental data reported in ref. [11]. It was shown that the resulting data-driven framework is then capable of utilizing both types of data via a single, fixed data set, which is computed in an offline step without the need of online adjustments. For load cycles for which no experimental data is available, the framework resorts to synthetic data. This synthetic data was created by alternating the load between 0 and a fixed value, as it was the case for the experimental load path. For an increasing density of the data sets, it was numerically shown in Figure 4 that the data-driven solution converges to the solution obtained via the conventional material model. The stress-strain solution, visualized in Figure 2, was compared qualitatively to the experimental data itself. For both cases, the data-driven framework provides accurate results. In Figure 2, the unloading path of the data-driven results deviated from the experimental data for the first cycle. This was credited to the chosen number of time steps and numerical weights, and should be able to be resolved by adjusting one or the other. This aspect should be considered in future work.

To conclude, the present contribution showcases the applicability of the data-driven approach to simulate the mechanical behavior under cyclic loading with application to SMA wires. The method allows for an incorporation of experimental data, if available, and provides a possibility to reduce the loss of information induced by resorting to material models alone. Due to the offline construction of the data set, new data can be included whenever it becomes available without the need of any additional adjustments. The extension of the data-driven mechanics method to path-dependent material behavior presents itself as a promising approach in the realm of computational mechanics, combining synthetic data obtained via classic material models with experimental data.

Utilizing the data-driven approach, the prediction of the behavior of SMA wires via ref. [10] is embedded into a finite element framework for truss structures. The data generation is already being designed such that it covers the data space encountered when such structures are subjected to prescribed loads the maxima of which are identical for each cycle. It is therefore conclusive to apply the presented framework to complex SMA (wire) structures in future work, which may allow for advanced applications.

ACKNOWLEDGMENTS

Financial support by the German Research Foundation (DFG) – Project-ID 440942664, Priority Programme 2256 "Variational Methods for Predicting Complex Phenomena in Engineering Structures and Materials" (project 3) – is gratefully acknowledged. Moreover, financial support by Vetenskapsradet (VR) – Project-ID 2022-03460, "Data-driven modeling of smart materials" – is gratefully acknowledged.

Open access funding enabled and organized by Projekt DEAL.

ORCID

Marius Harnisch https://orcid.org/0000-0003-3165-5459
Andreas Menzel https://orcid.org/0000-0002-7819-9254

REFERENCES

1. Kirchdoerfer, T., & Ortiz, M. (2016). Data-driven computational mechanics. *Computer Methods in Applied Mechanics and Engineering*, *304*, 81–101.
2. Ibanez, R., Abisset-Chavanne, E., Aguado, J. V., Gonzalez, D., Cueto, E., & Chinesta, F. (2018). A manifold learning approach to data-driven computational elasticity and inelasticity. *Archives of Computational Methods in Engineering*, *25*(1), 47–57.
3. Kirchdoerfer, T., & Ortiz, M. (2017). Data driven computing with noisy material data sets. *Computer Methods in Applied Mechanics and Engineering*, *326*, 622–641.
4. Bessa, M., Bostanabad, R., Liu, Z., Hu, A., Apley, D. W., Brinson, C., Chen, W., & Liu, W. K. (2017). A framework for data-driven analysis of materials under uncertainty: Countering the curse of dimensionality. *Computer Methods in Applied Mechanics and Engineering*, *320*, 633–667.
5. Leygue, A., Coret, M., Réthoré, J., Stainier, L., & Verron, E. (2018). Data-based derivation of material response. *Computer Methods in Applied Mechanics and Engineering*, *331*, 184–196.
6. Eggersmann, R., Kirchdoerfer, T., Reese, S., Stainier, L., & Ortiz, M. (2019). Model-free data-driven inelasticity. *Computer Methods in Applied Mechanics and Engineering*, *350*, 81–99.
7. Ciftci, K., & Hackl, K. (2022). Model-free data-driven simulation of inelastic materials using structured data sets, tangent space information and transition rules. *Computational Mechanics*, *70*, 425–435.
8. Poelstra, K., Bartel, T., & Schweizer, B. (2022). A data-driven framework for evolutionary problems in solid mechanics. *ZAMM - Journal of Applied Mathematics and Mechanics*, *103*(3), e202100538.
9. Bartel, T., Harnisch, M., Menzel, A., & Schweizer, B. (2023). Aspects of accuracy and uniqueness of solutions in data-driven mechanics. *Proceedings in Applied Mathematics and Mechanics*, *22*(1), e202200206.
10. Bartel, T., Osman, M., & Menzel, A. (2017). A phenomenological model for the simulation of functional fatigue in shape memory alloy wires. *Meccanica*, *52*, 973–988.
11. Eggeler, G., Hornbogen, E., Yawny, A., Heckmann, A., & Wagner, M. (2004). Structural and functional fatigue of NiTi shape memory alloys. *Materials Science and Engineering: A*, *378*(1–2), 24–33.
12. Bartel, T., Harnisch, M., Schweizer, B., & Menzel, A. (2023). A data-driven approach for plasticity using history surrogates: Theory and application in the context of truss structures. *Computer Methods in Applied Mechanics and Engineering*, *414*, 116138.

How to cite this article: Harnisch, M., Bartel, T., Weyergraf, L., Menzel, A., & Schweizer, B. (2024). Data-driven simulation of functional fatigue in shape memory alloy wires. *Proceedings in Applied Mathematics and Mechanics*, *24*, e202400079. https://doi.org/10.1002/pamm.202400079